Research Square

Preprints are preliminary reports that have not undergone peer review.
They should not be considered conclusive, used to inform clinical practice,
or referenced by the media as validated information.

Design and Simulation of a Differential MEMS Accelerometer with Interdigitated Triplet Fingers Based on a Novel SOI–Glass Bulk Microfabrication Scheme

S. Selvaraj

selvaraj.sitar@gov.in

Semiconductor Technology and Applied Research Centre (STARC)

K. Zaman Khan

Moscow Center for Advanced Studies, Kulakova str. 20,Moscow, Russia.

Vijaykumar SN

Semiconductor Technology and Applied Research Centre (STARC)

Thilak Gowda

Semiconductor Technology and Applied Research Centre (STARC)

S. Partheeban

Semiconductor Technology and Applied Research Centre (STARC)

Research Article

Keywords: Accelerometer, bulk-micromachining, fully differential capacitance, inter-digitated triplet fingers, high resistivity silicon. SOI wafer

Posted Date: November 13th, 2026

DOI: https://doi.org/10.21203/rs.3.rs-7911643/v1

License: This work is licensed under a Creative Commons Attribution 4.0 International License.
Read Full License

Additional Declarations: No competing interests reported.

Design and Simulation of a Differential MEMS Accelerometer with Interdigitated Triplet Fingers Based on a Novel SOI–Glass Bulk Microfabrication Scheme

S. Selvaraj[1#], K. Zaman Khan[2], Vijaykumar SN[1], Thilak Gowda A[1], S. Partheeban[1]
[1]Semiconductor Technology and Applied Research Centre (STARC), Bangalore, India.
[2] Moscow Center for Advanced Studies, Kulakova str. 20, Moscow, Russia
[#] email: selvaraj.sitar@gov.in

Abstract:

A novel microfabrication scheme based on SOI-glass bulk micromachining technique is proposed for realizing a single axis MEMS differential accelerometer with inter-digitated triplet fixed fingers. In this method, the fixed fingers are anchored all along their length to avoid their movement in response to the applied acceleration. This overcomes sensitivity degradation, which is undesired in high performance accelerometers. SOI wafer with 100 µm thick device layer is suggested for forming the proof mass. Width of the fixed fingers is chosen to be 100µm to enable wafer bonding and electrically access the fixed fingers through the wafer-bonded interface. Partial sacrificial release etch of buried oxide under fixed fingers ensures sufficient anchoring. Retention of the handle layer provides a robust stopper mechanism. The single axis acceleration sensor is modelled and designed for a range of 100g, based on the proposed process scheme. Simulations were carried out using Coventorware design software. Simulation result shows that the first mode frequency is 4481 Hz which is beyond normal system vibration frequencies as desired. Electromechanical simulations demonstrated a capacitance sensitivity of 3.1 fF/g with a linear response of 0.11%FS. The salient feature of the process scheme compared to other reported processes is that the devices fabricated will provide stoppers and completely fixed fingers with electrical access through wafer bonding interface, simplifying the packaging. Utilizing a SOI wafer with thick buried oxide and high resistivity silicon handle layer will further minimize the parasitic effects.

Keywords— Accelerometer, bulk-micromachining, fully differential capacitance, inter-digitated triplet fingers, high resistivity silicon. SOI wafer

Introduction:

Improvement in acceleration sensing is always a need of continuous development in modern science and technology to meet a wide variety of emerging applications. There are multiple methods of sensing acceleration based on different transduction techniques; capacitive, piezoelectric, piezoresistive, thermal, and tunnelling [1]. Each technique has advantages and disadvantages due to unique features and hence sensor based on a single technique cannot meet all application requirements. Among the above transduction methods, capacitive accelerometers have relative advantage due to low power consumption, less temperature dependence, suitability for measuring both static and dynamic acceleration [2-3]. MEMS capacitive accelerometers have many applications, including in automobiles, consumer electronics, gaming, guidance systems and navigation [4-5]. Movement of proof mass in an accelerometer produces capacitance change Δc in response to applied acceleration and the Δc is interpreted as a measure of acceleration [2,5-6]. Gap change sense approach is preferred over area change sense approach due to improved sensitivity [7]. Linearity issues arising

due to gap change approach can be addressed in design with differential capacitance configuration and also optimizing the displacement of proof mass. Accelerometer with differential capacitance structure has major benefits in terms of Common Mode Rejection Ratio (CMRR), Power Supply Rejection Ratio (PSRR) improvement [8-10]. Electrically isolated proof masses with differential structure has been proposed by researchers for realizing fully differential interface circuit and improving sensitivity while reducing parasitic capacitances [1,11]. Inter-digitated comb fingers of parallel plate capacitive detection based on gap change is used in a fully differential interface circuit. Differential finger configuration with interdigitated triplet fingers have more advantages compared to fingers with gap/anti-gap configurations. Interdigitated triplet finger configuration provide excellent CMRR and suitable for force feedback closed loop circuit required for high performance accelerometers. In this context interdigitated triplet finger structure is preferred for acceleration sensors. Normally, surface micromachining technique provides easiest way of fabricating in-plane accelerometers with interdigitated triplet finger structure. Fully differential structure realized using surface micromachining, especially metal based, has inherent problems due to buckling, low resolution due to smaller mass and less sensitivity due to thinner proof mass. [12-13].

MEMS accelerometers with a small mass also limits the minimum detectable acceleration due to mechanical Brownian noise [14-15]. To achieve low mechanical noise heavier proof mass is required [16], which is practically difficult to realize using surface micromachining technique. These issues can be improved using bulk micromachining [16-17]. However, the advantages of thicker proof mass in bulk micromachining is counter-productive due to increased gap, caused by process limitations[16]. To increase the sensitivity of accelerometers and for improved performance in closed loop operation, interdigitated triplet finger configurations have been suggested [17-20]. To avoid problems arising due to glass proof mass [20] and less anchor area for the interdigitated fingers realized in SOI wafers [21], researchers have realized interdigitated triplet fingers using wafer bonding of SOI wafer with metallized glass wafer and taking metal contact through buried oxide contact opening[16]. The scheme of interdigitated triplet finger configuration and electrical access proposed as per [16] is illustrated in figure 1. To minimize parasitic capacitance effect handle layer can be removed [20].

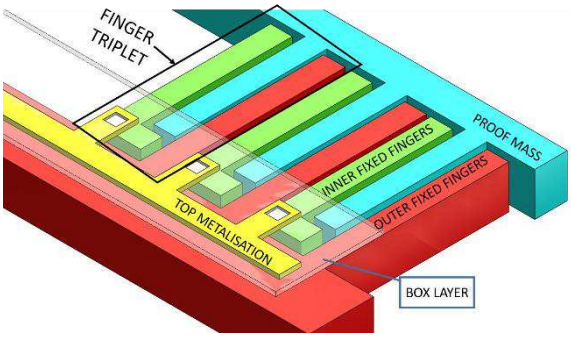


Figure 1: Structure of interdigitated triplet fingers[16]

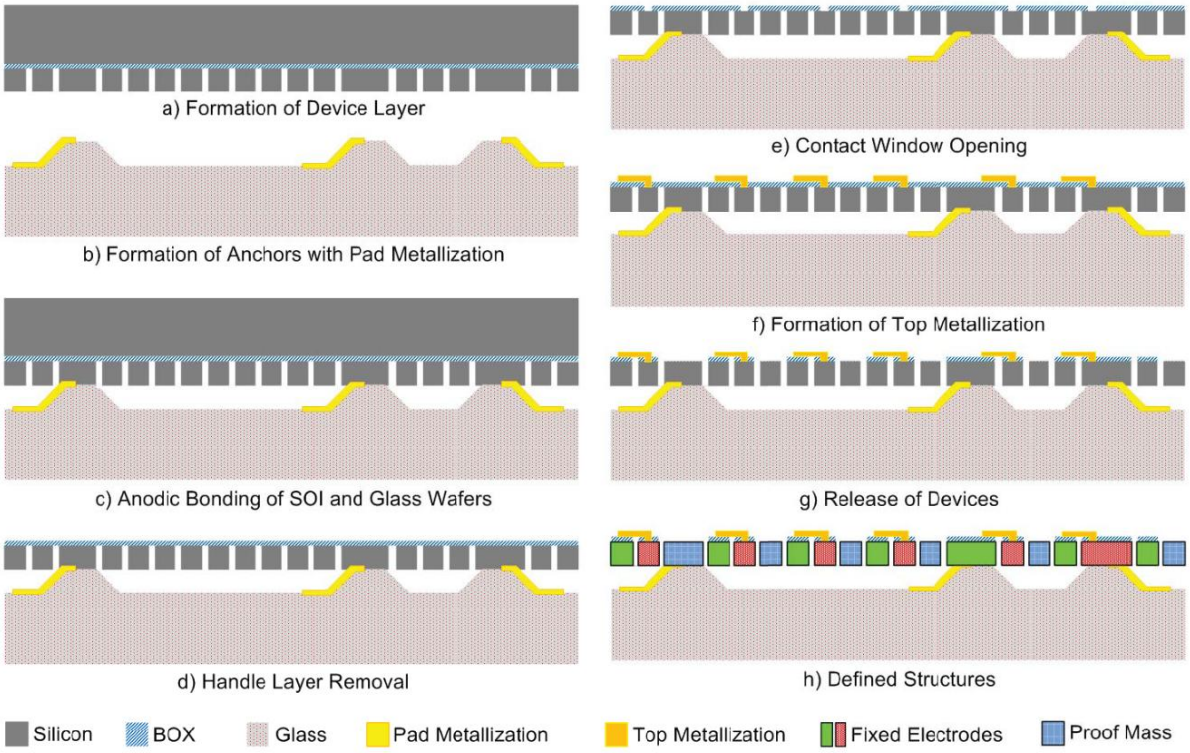


Figure 2: SOI wafer based bulk micromachining process flow [16]

It is not straight forward to fabricate the interdigitated triplet structure with proper metal connections using bulk micromachining (SOI route) as compared to surface micromachining technique. The interdigitated triplet fingers structure using SOI-glass wafer based bulk micromachining has been successfully fabricated by researchers [16] using Silicon-on-Glass (M-SOG) process developed at METU-MEMS Center [22]. The fabrication process flow adopted in [16] is illustrated in figure 2. The interdigitated triplet structure in their research was achieved through wafer bonding of SOI wafer and metalized glass wafer. As shown in figure 1, the inner / outer finger sets have been metallized from the top by opening buried oxide and then depositing metal. Since the handle layer has been removed after bonding with glass wafer as shown in figure 2, the buried oxide is visible from the top as illustrated in figure 1, with the device layer, on which fingers are formed, is at the bottom. The glass wafer below the device layer is also not visible in the figure 1. The buried oxide provides necessary isolation between inner fingers, outer fingers and proof mass. Metal connections to the fingers and proof mass could not be taken through metal contact at glass wafer bonding interface for the process flow given in figure 2, as width of fixed and moveable fingers were 5 µm and 7 µm, respectively with a gap of 3 µm between them. It is to be noted that the bonding strength at anchoring site of the fixed combs in the interdigitated triplet structure realized in this manner is weak, due to small bond area. The weak bonding at the anchoring of the fingers will cause reliability concern especially for high performance accelerometers. The fixed fingers are anchored only at the ends of the fingers. As a result, the fixed fingers will act as free cantilevers and undergo deflection under acceleration causing reduction in sensitivity [1]. Hence, it would be beneficial if the fixed fingers are anchored all along their length. There is also no option for providing stopper in the accelerometers reported at ref. [16].

This paper proposes an alternative process method using SOI-glass wafer based on bulk micromachining technique for realizing interdigitated triplet structure with fixed fingers rigidly anchored all along their length. This approach also enables taking electrical access via glass-silicon bond metal interface and formation of stoppers. Details of design and simulation of a single axis in plane acceleration sensor based on proposed process method are reported in this paper.

A. Proposed Process Method

The proposed process method suggests the use of Silicon on Insulator (SOI) and glass wafers for fabrication of MEMS acceleration sensor with novel scheme for realizing interdigitated triplet fingers. The process consists of three main segments namely; (i) SOI wafer processing; (ii) glass wafer processing; (iii) Combining processed SOI and glass wafers. Tentative process sequences are illustrated in figure 4.

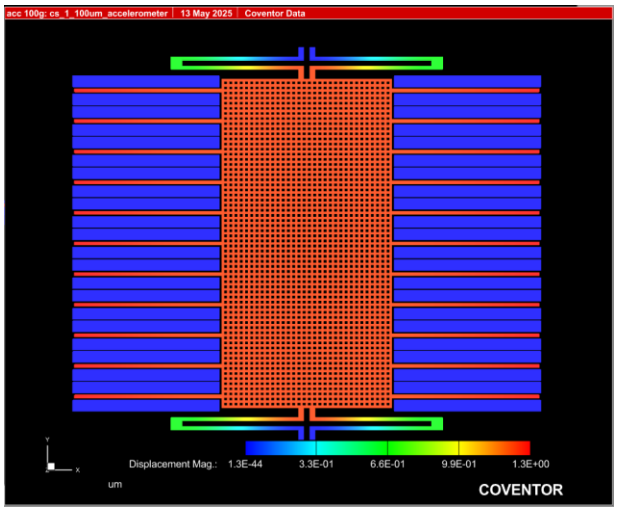


Figure 3: Topology of acceleration sensor as per process method proposed in this research

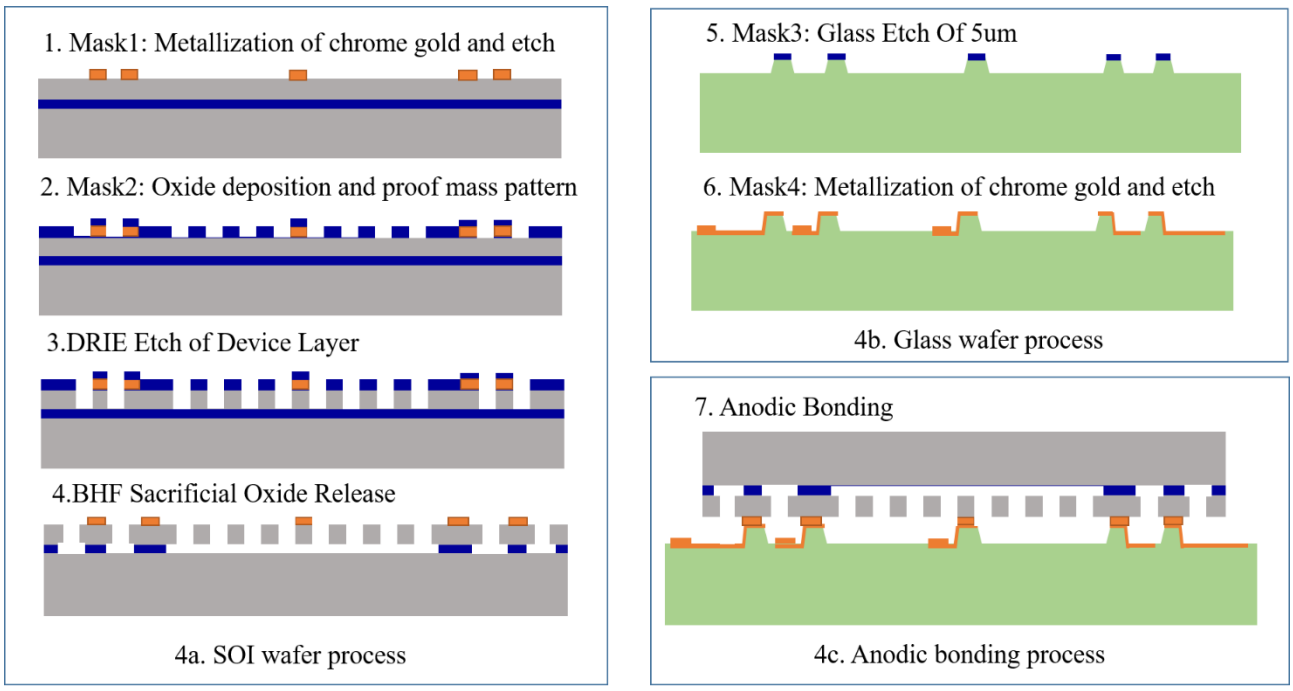


Figure 4: SOI-glass wafer bulk micromachining process flow proposed in this report

Device layer thickness of 100 µm is proposed for realizing silicon MEMS structures namely; proof mass, fixed, and moveable fingers. Folded beam is considered for the spring structure. The topology of acceleration sensor considered for present study is as shown in figure 3. Width dimension of 100 µm for fixed fingers is chosen in order to increase the bond area. Other dimensions of the MEMS structures as shown in table 1.

(i) SOI wafer processing:

The process on SOI wafer starts with metallization of device layer with a stack of chrome and gold. Metal stack is etched using Mask 1 pattern as shown in figure 4a. Oxide layer of thickness 1µm - 2 µm is deposited over the patterned metal followed by patterning and etching using proof mass pattern Mask 2. The oxide layer with proof mass pattern serves as a hard mask during Deep Reactive Ion Etching(DRIE) to create the proof mass in the device layer. Subsequently, sacrificial etch process using BHF solution releases the proof mass. The perforations on the proof mass facilitate etching of the underneath buried oxide layer. The entire SOI wafer processing requires two patterning (masking) steps.

(ii) Glass wafer processing:

The glass wafer processing is performed separately as illustrated in figure 4b. A cavity etch of depth ~5µm as per pattern Mask 3 is created in the glass wafer. Chrome-gold layer is then deposited and etched as per pattern Mask 4 for tracks leading to wire bond pads. Two masks are required for glass processing.

(iii) Combined wafer processing:

Both the processed wafers are bonded using anodic bonding method (figure 4c). The glass die layout is larger than silicon die layout to accommodate wire bond pads. Figure 5 depicts sketch of the MEMS acceleration sensor die layout. The handle layer is not removed in this process to realize the stopper.

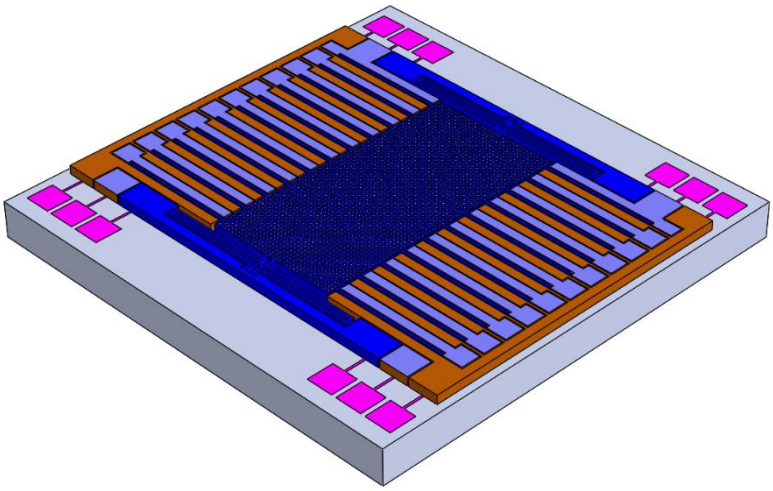


Figure 5: 3D model of single axis accelerometer built based on the proposed process flow (handle layer hidden)

B. Design and Simulation

An acceleration sensor design has been implemented in Coventorware design software using layout as per dimensions given in table 1. The device design was carried out for acceleration range 0-100g. Folded beam design is used for the springs. Analytical calculation of spring constant and frequency of spring mass system is done to roughly estimate suitable dimensions using the equations (1) and (2). Simulation results are used for comparison and verification purpose. Dimensions are targeted such that the first mode frequency is above system vibration frequency which is normally around 2000 Hz. The calculation of frequency using the dimensions given in table 1 gives the first model frequency to be 3757 Hz which is meeting the above requirement. Mass of the proof mass and spring constant values are estimated to be 0.94µg and 527 N/m respectively.

$$f = \frac{1}{2\pi}\sqrt{\frac{K}{m}} \quad \text{Hz} \qquad \text{-------- (1)}$$

Where 'K' is spring constant and 'm' is the mass.
The spring constant K is given by

$$K = \frac{Etw^3}{2l^3} \quad \text{N/m} \qquad \text{--------- (2)}$$

Where E = Young's Modulus of Silicon = 130 GPa; t = thickness of spring = 100 µm; w = width of the spring beam = 30µm; l = length of spring (length of single beam = 1100µm).

Table 1: Dimensions of proof mass used for design & simulation

Structural elements	**Dimension in µm**
Proof mass	
Size in x direction	1500
Size in y direction	2900

Hole size	25
Line width	20
Moveable Comb finger	
Length	1300
Width	30
Fixed fingers	
Length	1300
Width	100
Gap Between Fingers	
Fixed-fixed; fixed-moveable	15
Spring Beam	
Width	30
Length	1100
Width of connecting beam	40
Length of connection beam	100

A 3D model is built in Coventorware design software by combining the process flow and layout dimensions given in table 1. Fixed boundary conditions are applied appropriately. Simulation is carried out to find out the modal frequency of the accelerometer. The first mode frequency of the acceleration sensor is found to be 4481 Hz as per simulation. Figure 5 shows simulation results for frequencies for 6 modes of vibration.

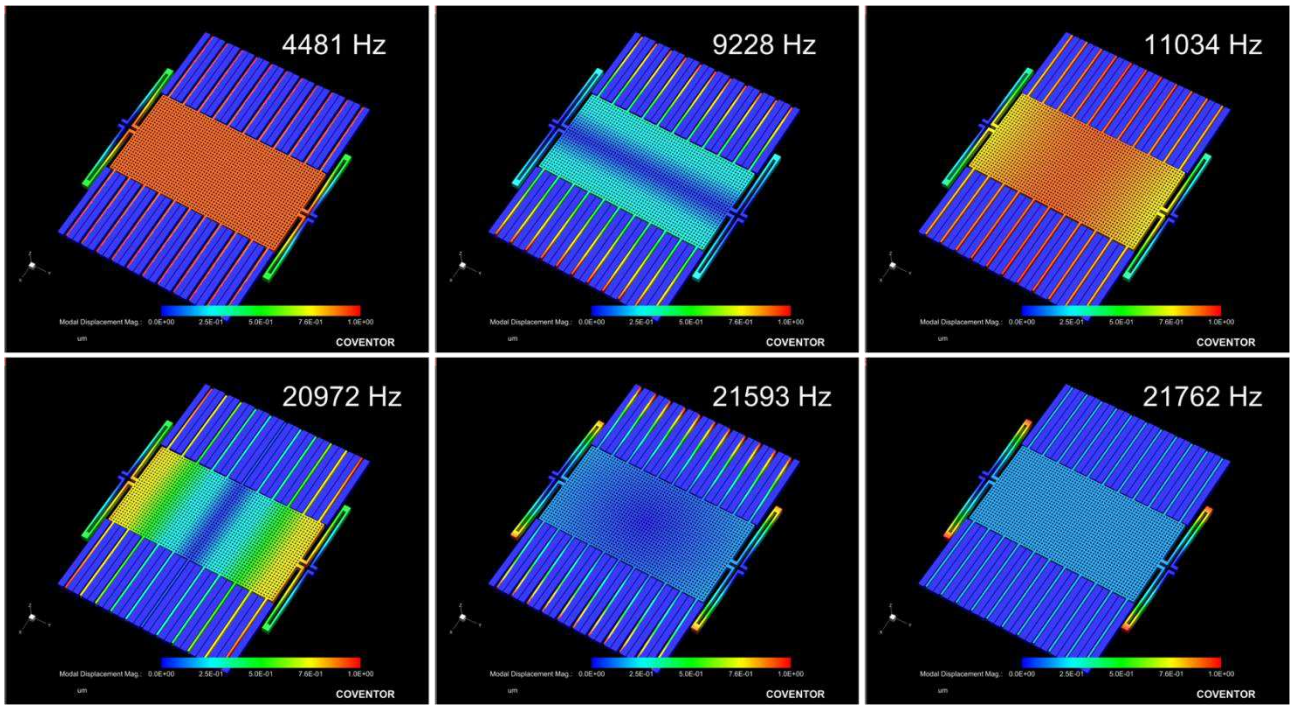


Figure 6: Mode shapes of acceleration sensor (6 modes)

Mechanical Simulations

Mechanical simulations were further carried out to study the performance of acceleration sensor. Acceleration was applied from 0 to 100g along the sense axis (y-axis) to determine proof mass

displacement as a function of applied acceleration. Figure 7 shows acceleration versus displacement graph. Maximum stress induced due to the proof mass displacement is 7.8 MPa which is much lesser than the Yield strength of Silicon (7 GPa).

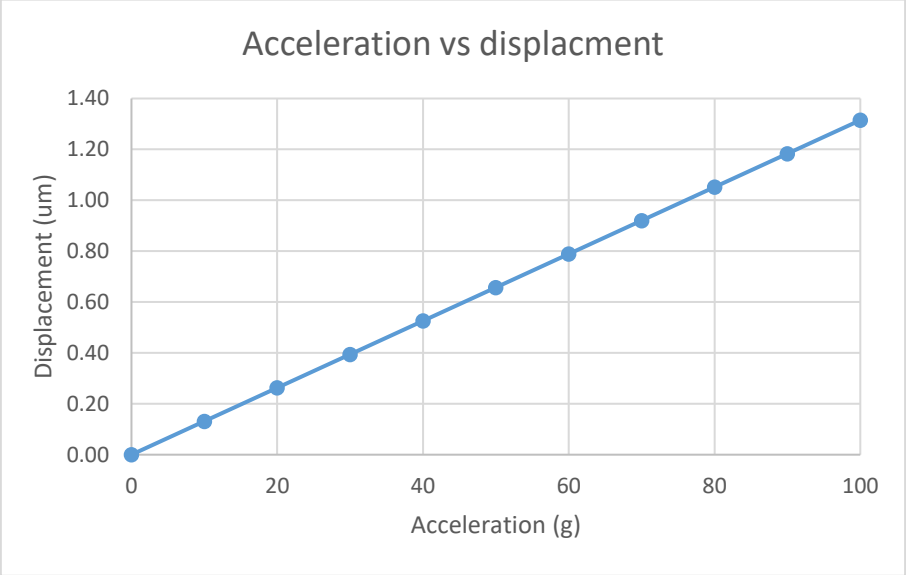


Figure 7: Proof mass displacement versus acceleration

Electrical simulations

Base capacitance between moveable and fixed combs is analytically estimated to be 0.8 pF. Total capacitance (including fringe capacitance) is found to be 1.8 pF. Coupled analysis is carried out by coupling the mechanical displacement result obtained from Coventorware with electrical domain. The simulation result for delta capacitance variation as function of applied acceleration is shown in figure 8. Calculation of non-linearity from this graph using residuals yields a value of 0.11% & sensitivity value is found to be 3.1 fF/g.

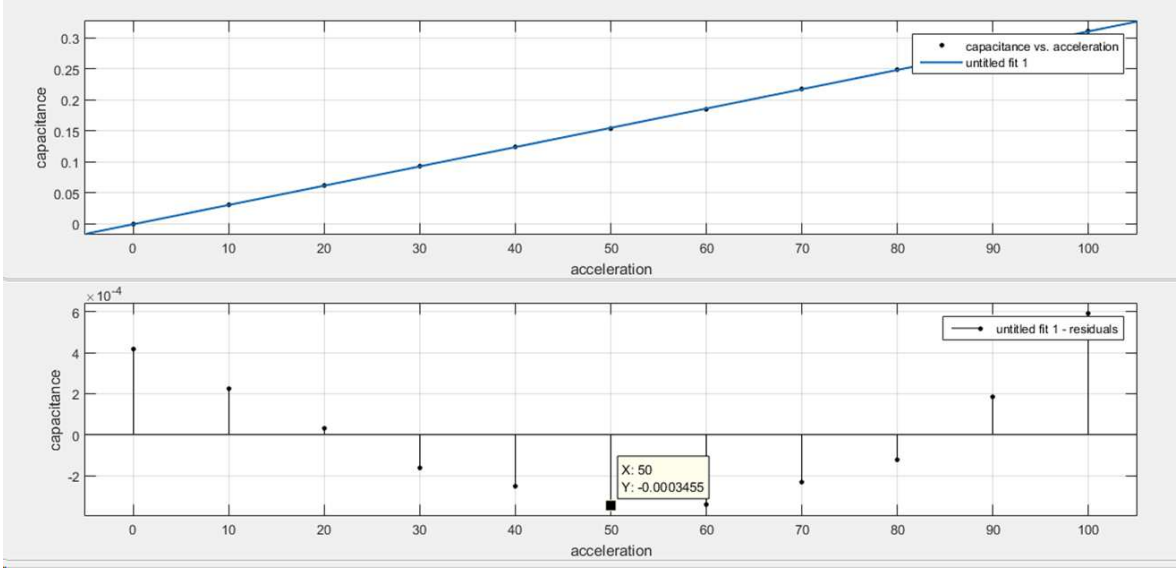


Figure 8: Delta Capacitance variation as a function of applied acceleration

Pull-in voltage for the structure is calculated using equation (3).

$$V_{pullin} = \sqrt{\frac{8Kd^3}{27\varepsilon_0 A_f}}$$

---------- (3)

Where K= 527 Nm^{-1} is the spring constant, d = 15µm is the gap between fingers; ε_o= 8.85 x 10^{-12} F/m is the absolute free space permittivity, A_f= ~2.86 x 10^{-6} m^2 is the cross sectional area of the fingers corresponding to 22 moveable fingers.

Pull-in voltage as per calculations is 144.3V and simulated value is found to be about 160 V (figure 9). Parasitic value is arising majorly due to retaining of the handle layer. Parasitic capacitance values for buried oxide thickness of 1µm and 6µm are 159 pF and 26.5 pF respectively.

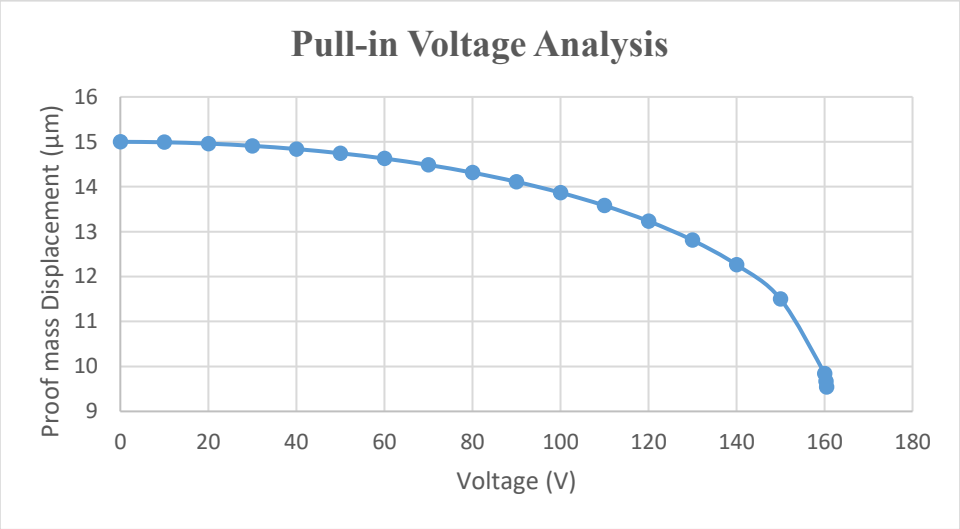


Figure 9: Pull-in analysis

Damping analysis

Squeeze film damping and slide film damping will have major influence on the dynamic performance of the acceleration sensor. Squeeze film damping coefficient for the present design is calculated using equation (4).

$$b_1 = N_f \mu_{eff} l_f \left(\frac{t}{d_o}\right)^3 \quad \text{…….. (4)}$$

Where, N_f = 22 is the number of moveable combs; μ_{eff} = 18.5 x 10^{-6} Ns/m^2 is the effective viscosity of air=; l_f= 1100 µm is the length of fingers ; t= 100µm is the thickness of the fingers; d_0 = 15µm is the gap between fingers.

Slide film damping coefficient is calculated using the formula (5).

$$b_2 = \mu_{eff} \frac{A}{d} \quad \text{…… (5)}$$

Where A = sum of planar area of proof mass and planar area of 22 fixed fingers.

Total damping is $b = b_1 + b_2$ …… (6)

Damping ratio (ζ), raising time (t_r) and settling time (t_s) for the design are calculated respectively using the equations (7), (8), and (9).

$$\zeta = \frac{b}{2m\omega_n} \quad \text{..... (7)}$$

$$t_r = \frac{\pi - tan^{-1}\frac{\sqrt{1-\zeta^2}}{\zeta}}{\omega_n\sqrt{1-\zeta^2}} \quad \text{---------- (8)}$$

$$t_s = \frac{4}{\omega_n\zeta} \quad \text{---------- (9)}$$

Calculated values of damping parameters are given in table 2.

Table 2: Calculated damping parameters

b	1.57×10^{-4}	N s/m
ζ	0.00395	-
t_r	66.703	us
t_s	42.89	ms

C. Results and Discussion

The proposed process method is expected to allow fabrication of acceleration sensor with fully differential interdigitated triplet structure with enhanced structural capability. The new process method enables fabrication of the sensor using just 4-5 masks compared to previous report [16]. The sensor uses wide fixed fingers to enable taking electrical contact from the silicon-glass bond area which was a limiting issue for the process used in ref [16] due to very less area of bonding. The proof mass is released using sacrificial etch process. The perforations on the proof mass permits the etchants to reach out to the underneath buried oxide below proof mass. The line width between perforations 20µm. Hence, an undercut over 10µm will enable complete removal of the buried oxide below the proof mass. However, the device is completely released only if oxide under the connecting bar in the spring having the largest width of 40µm is released. This would require an over etch of 20µm - 25µm. At this juncture, the buried oxide below the wide fixed fingers would not be completely etched, leaving effectively at least 50µm buried oxide underneath the fingers. This is the salient feature of the proposed process method as the 50µm buried oxide below the fixed fingers provide anchoring all along their length. In addition the fixed fingers are also anchored at glass-silicon bond surface. As a result, the cantilever movement of the fixed fingers in response to applied acceleration, which occurs in sensors realized by researchers [16], can be avoided. This is beneficial as cantilever movement of fixed fingers is unwanted and leads to sensitivity degradation [1]. Another important feature is that retaining the handle layer of the SOI wafer after wafer bonding is helpful to realize stopper. However, effect of parasitic capacitance and ways to mitigate it have to be further studied.

3D model of the combined wafers of a die is shown in figure 10. Expected die size is around 5mm x 5mm x 1mm. Wire bond pads are placed on the glass wafer. One set of fixed fingers (Elec. 1) are electrically shorted in the device layer silicon itself. Metal pad on device silicon is electrically connected to the wire bond pad (A) on glass through wafer bond metal interface as shown in figure 10. The other set of fixed fingers (Elec.2) are electrically shorted using metal routing via wafer bond

metal interface on glass wafer. Elec.2 electrode is connected to the wire bond (B) on the glass wafer. Pad on proof mass (Elec. 3) is electrically connected to the wire bond pad (C) on glass wafer via wafer bond metal interface.

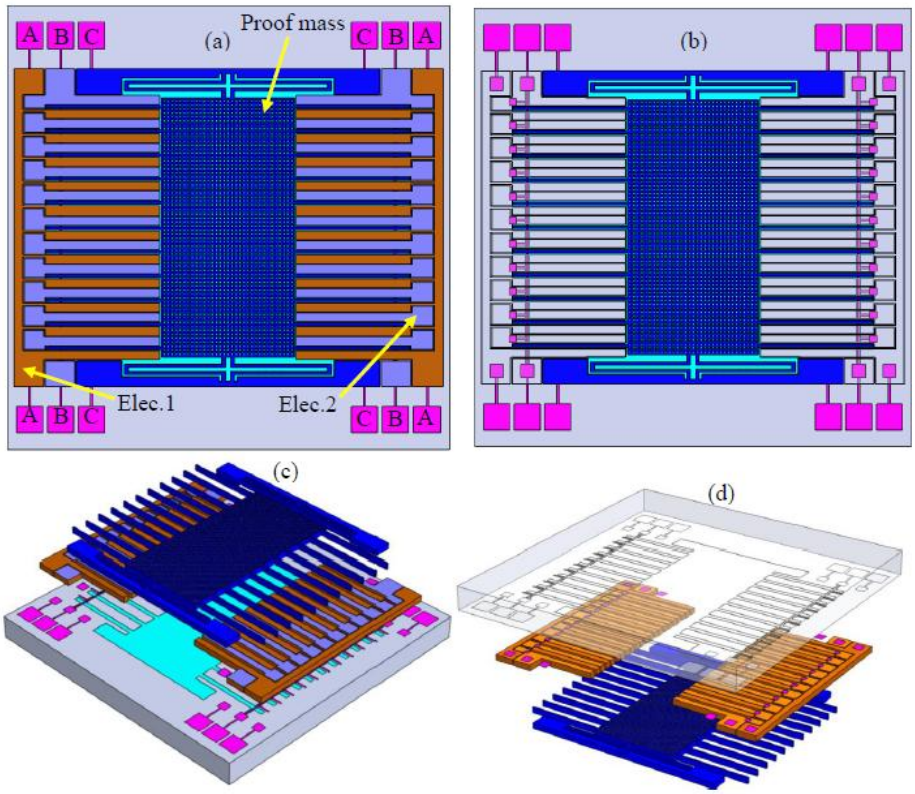


Figure 10: Schematic of die 3D layout as per proposed process method. Die Size ~ 5mm × 5 mm × 1mm (a) Top side view; (b) Bottom view (with glass transparent); (c) Exploaded view (topside); (d) Exploaded view (bottom side) – handle layer hidden

First mode frequency values obtained through analytical method and simulation are respectively 3757 Hz and 4481 Hz. The difference between analytical and simulated results is found to be ~16%.

Simulation result at figure 7 shows linear behaviour of proof mass displacement as a function of acceleration. Maximum displacement of the proof mass is found to be ~ 1.09µm for 100g acceleration which is less than 15% of finger gap, which is 15µm, as required by accelerometer design principle [16]. Mechanical factor of safety based on maximum stress (7.8 Mpa) induced by the applied acceleration is found to be around 900 and thus the design has high safety margin.

The graph in figure 8 shows linear behaviour of delta capacitance variation as a function of acceleration. Non-linearity value calculated from maximum residue plot is 0.11%, and sensitivity is found to be 3.1 fF/g, which is good for further processing. Similar sensitivity values have been reported in earlier work [23]. Pull-in voltage values obtained from analytical calculation (144 V) and simulated (160 V) values are also comparable. This establishes that the sensor can provide stable performance.

Parasitic capacitances effects need to be addressed as handle layer is not removed in the present design. Parasitic capacitance can be minimized by using thick buried oxide in the SOI wafer. Parasitic

capacitance values with buried oxide thickness of 1 μm & 6 μm are 159 pF and 26.5pF respectively. Parasitic capacitance can be minimized by using SOI wafer with higher buried oxide thickness of 6μm. It is also possible to reduce the parasitic capacitance effect if handle layer with high resistivity in the order of 10 kOhm.cm is used. Based on application requirements, option for handle layer removal also can be considered for minimizing parasitic capacitance if stopper is avoidable.

Combined effect of squeeze film damping and slide film damping has been considered in the analysis. Calculated values of damping coefficient and damping ratio are given in table 2. Estimated values for Rise time t_r and settling time t_s are found to be 66.7μs and 42.89 ms.

D. Conclusions

This paper has presented a new method of realizing in plane acceleration sensor with interdigitated triplet configurations using SOI-glass wafer bulk micromachining with enhanced features. Number of masks required for fabrication is reduced compared to process flow reported earlier[16]. The process method provides salient feature of anchoring of fixed fingers all along their length to avoid sensitivity degradation. Possibility of realizing stopper mechanism is another advantage. Parasitic capacitance effect can be minimized by selecting SOI wafers with thick buried oxide layer. Use of high resistivity (10 kohm.cm) handle layer silicon can be also considered to minimize the parasitic capacitance. Acceleration sensor design based on the proposed process method yields reasonable performance parameters like, modal frequency of 4481 Hz, non-linearity of 0.11%, sensitivity of 3.1 fF/g. High electrical pull-in voltage provides stable operation. The device with thick device layer (100 μm) is expected to have rugged performance with high factor of safety (900) suitable for high end applications, such as defese and aerospace applications. Damping analysis suggests that the sensor would provide good dynamic behaviour. Acceleration sensor developed based on this approach after integrating with suitable read-out circuit is expected to deliver enhanced performance.

Declarations

The authors have no conflicts of interest to declare that are relevant to the content of this article.

References

1. Mansour Keshavarzi, Javad Yavand Hasani, "Technical Paper on : Design and optimization of fully differential capacitive MEMS accelerometer based on surface micromachining" , Microsystem Technologies, © Springer-Verlag GmbH Germany, part of Springer Nature 2018, Published online: 17 Oct.2018; https://doi.org/10.1007/s00542-018-4187-5

2. Mohammed et al. 2017- Mohammed Z, Dushaq G, Chatterjee A, Rasras M, "An optimization technique for performance improvement of gap- changeable MEMS accelerometers", . Mechatronics. https://doi. org/10.1016/j.mechatronics.2017.10.011;

3. Yazdi N, Ayazi F, Najafi K (1998), "Micromachined inertial sensors", Proc IEEE. https://doi.org/10.1109/5.704269

4. Zhou X, Che L, Wu J, Li X, Wang Y (2012), “A novel sandwich capacitive accelerometer with a symmetrical structure fabricated from a D-SOI wafer”. J Micromech Microeng 22(8):85031. https://doi.org/10.1088/0960-1317/22/8/085031

5. Xiao D, Li Q, Hou Z, Xia D, Xu X, Wu X (2017) A double differential torsional micro-accelerometer based on V-shape beam. Sens Actuators A 258(May):182–192. https://doi.org/10.1016/j.sna.2017.03.011

6. Kavitha S, Joseph Daniel R, Sumangala K (2016), “Design and analysis of MEMS comb drive capacitive accelerometer for SHM and seismic applications”. J Meas 93(November):327–339. https://doi.org/10.1016/j.measurement.2016.07.029

7. Szermer M, Nazdrowicz J, Zabierowski W (2017) FEM analysis of a 3D model of a capacitive surface-micro machined accelerometer. In: 2017 14th international conference the experience of designing and application of CAD systems in microelectronics (CADSM). IEEE, New York, pp 432–34. https://doi.org/10.1109/cadsm.2017.7916168

8. Ru Li, Zakriya, Mahamoud Rasras, Ibrahim (Abe) M.Elfadel, Daniel Choi, “Design, modelling and characterization of comb drive MEMS gap-changeable differential capacitive accelerometer”, Measurement 169 (2021), 108377.

9. Benmessaoud M, Nasreddine MM (2013) Optimization of MEMS capacitive accelerometer. Microsyst Technol 19(5):713–720. https://doi.org/10.1007/s00542-013-1741-z

10. Hsu YC, Lin CW, Sun CM, Hsu CP, Lee YT, Tsai MH, Liu YC, Fang W (2011) Implementation of fully-differential capacitance sensing accelerometer using glass proof-mass with SI-VIAS. In: Proceedings of the IEEE international conference on micro electro mechanical systems (MEMS), January. IEEE, New York, pp 589–592. https://doi.org/10.1109/memsys.2011.5734493

11. Luo H, Zhang G, Carley LR, Fedder GK (2002) A post-CMOS micromachined lateral accelerometer. J Microelectromech Syst 11(3):188–195. https://doi.org/10.1109/JMEMS.2002.1007397

13. Osman Aydin and Tayfun Akin, “A Bulk-Micromachined Fully Differential MEMS Accelerometer With Split Interdigitated Fingers”, IEEE SENSORS JOURNAL, VOL. 13, NO. 8, AUGUST 2013, page 2914-2921.

12. Y. C. Hsu, C. W. Lin, C. M. Sun, C. P. Hsu, Y. T. Lee, M. H. Tsai, Y. C. Liu, and W. Fang, “Implementation of fully-differential capacitance sensing accelerometer using glass proof-mass with Si-vias,” in Proc. IEEE Int. Conf. Micro Electro Mech. Syst., Jan. 2011, pp. 589–592.

13. H. Luo, G. K. Fedder, and L. R. Carley, “A 1 mG lateral CMOS-MEMS accelerometer,” in Proc. IEEE Int. Conf. Micro Electro Mech. Syst., Jan. 2000, pp. 502–507.

14. A. Wung, R. V. Park, K. J. Rebello, and G. K. Fedder, “Tri-axial high-g CMOS-MEMS capacitive accelerometer array,” in Proc. IEEE Int. Conf. Micro Electro Mech. Syst., Jan. 2008, pp. 876–879.

15. Kalyan Kumar Mistry, K.B.M. Swamy, Siddhartha Sen, “Design of SOI-MEMS high resolution capacitive type single axis accelerometer”, Microsyst. Technol.(2010), 16:2057-2066, DOI: 10.1007/S00542-010-1146-1.

16. Osman Aydin and Tayfun Akin, A Bulk-Micromachined Fully Differential MEMS Accelerometer With Split Interdigitated Fingers, IEEE SENSORS JOURNAL, VOL. 13, NO. 8, AUGUST 2013, 2914-21.

17. J. B. Starr, “Squeeze-film damping in solid-state accelerometers,” in IEEE 4th Tech. Dig. Solid-State Sensor Actuator Workshop, Jun. 1990, pp. 44–47,

18. Y. Tang and K. Najafi, “High aspect-ratio low-noise multi-axis accelerometers made from thick silicon,” in Proc. IEEE Int. Symp. Inertial Sensors Syst., Feb. 2016, pp. 121–124.]

19. R. Abdolvand, B. V. Amini, and F. Ayazi, “Sub-micro-gravity in-plane accelerometer with reduced capacitive gaps and extra seismic mass,” IEEE J. Microelectromech. Syst., vol. 16, no. 5, pp. 1036–1043, Oct. 2007.

20. Y. C. Hsu, C. W. Lin, C. M. Sun, C. P. Hsu, Y. T. Lee, M. H. Tsai, Y. C. Liu, and W. Fang, “Implementation of fully-differential capacitance sensing accelerometer using glass proof-mass with Si-vias,” in Proc.IEEE Int. Conf. Micro Electro Mech. Syst., Jan. 2011, pp. 589–592.

21. G. G. Li, B. Gogoi, H. D. Desai, J. H. Hammond, and B. Diem, “MEMS device and method of fabrication,” U.S. Patent 0 090 474, Apr. 26, 2007.

22. M. M. Torunbalci, E. Tatar, S. E. Alper, and T. Akin, “Comparison of two alternative silicon-on-glass microfabrication processes for MEMS inertial sensors,” Proc. Eng., vol. 25, pp. 900–903, Sep. 2011.

23. Sinha S, Shakya S, Mukhyia R, Gopal R, Pent BD, “ Design and simulation of MEMS differential capacitive accelerometer”, (2014), In Proceedings of ISSS international conference on Smart materials, structures and systems, July 8-11, 2014, Bangalore, India.